Journal of Power Sources 196 (2011) 10050–10056

Contents lists available at SciVerse ScienceDirect

Journal of Power Sources

journal homepage: www.elsevier.com/locate/jpowsour

A simple, analytic model of polymer electrolyte membrane fuel cell anode recirculation at operating power including nitrogen crossover

Keith Promislow [a], Jean St-Pierre [b], Brian Wetton [c,*]

[a] Mathematics Department, MSU, United States
[b] Hawaii Natural Energy Institute, University of Hawaii at Manoa, United States
[c] Mathematics Department, UBC, Canada

ARTICLE INFO

Article history:
Received 22 June 2011
Received in revised form 14 August 2011
Accepted 16 August 2011
Available online 22 August 2011

Keywords:
PEMFC
Nitrogen crossover
Anode recirculation
Modelling
Optimization

ABSTRACT

A simple, analytic model is presented that describes the steady state profile of anode nitrogen concentration in a polymer electrolyte membrane fuel cell operated with anode recirculation. The model is appropriate for fuel cells with straight gas channels and includes the effect of nitrogen crossover from cathode to anode through the membrane. The key analytic simplification in the model is that this crossover rate, when scaled to the gas flows in the channels, is small. This is a good approximation when the device is used at operating power levels. The model shows that the characteristic times for the anode nitrogen profiles to reach steady state are of the order of minutes and that the dilution effect of anode nitrogen is severe for pure recirculation. The model shows additionally that a small anode outlet bleed can significantly reduce the nitrogen dilution effect. Within the framework of the model, the energy efficiency of pure recirculation can be compared to hydrogen venting or partial anode bleeding. An optimal bleed rate is identified. The model and optimization analysis can be adapted to other fuel cell designs and operating conditions. Along with operating conditions, only two key parameters are needed: a nitrogen crossover coefficient and the marginal efficiency loss to compressors for increased anode stoichiometric gas flow.

1. Introduction

Polymer electrolyte membrane fuel cells (PEMFCs) are a promising technology for power production. They combine anode fuel (pure hydrogen, methanol, or various reformates) with cathode oxidant (air or enriched air) in a catalysed electrochemical reaction that produces electrical energy. See [16] for a general reference.

Using pure hydrogen as an anode fuel has many advantages: anode kinetic losses are very low with this fuel compared to methanol [17], and the byproducts of reformate such as CO that can poison the anode kinetics are not present [26]. There are efficiency losses to venting excess hydrogen at anode outlet. These losses can be reduced by lowering the anode flow rate. However, when the anode stoichiometric flow rate is near one, there is increased risk of anode outlet starvation, which is a major source of cell degradation [8]. There are strategies to avoid having hydrogen exit the PEMFC system. The anode can be dead-ended (no outlet flow) [14,19,20] as in the Ballard Nexa design [29] and some recent air-breathing designs [9,12,18]. However, this strategy can require a mechanism to counteract anode nitrogen build-up at outlet. This nitrogen reaches the anode by crossing through the membrane from the cathode which has nitrogen from the ambient air used as the source for the oxidant gas [2]. An alternative strategy to venting or dead-end operation is anode recirculation [1,3–5,15,22]. Anode outlet gases, including unused hydrogen, are added back into the anode inlet along with additional hydrogen to maintain a given stoichiometric flow rate. Recirculation is compared to the other anode outlet strategies graphically in Fig. 1. Both pure recirculation and dead-end operation can be modified with partial anode outlet flow bleed. Like dead-end operation, recirculation is subject to anode nitrogen build-up due to crossover. The crossover rate is typically small but over time anode nitrogen concentrations in recirculating systems will build until they are comparable to those in the cathode. This dilution effect of anode hydrogen by nitrogen is demonstrated quantitatively in the present paper. In addition to this dilution effect, the efficiency of the cell is reduced due to the parasitic losses of the compressors recirculating the additional anode nitrogen flow. In this paper, we present a simple model of the build-up of nitrogen in the anode under recirculation. The model

* Corresponding author. Tel.: +1 604 822 5784; fax: +1 604 822 6074.
E-mail addresses: kpromisl@math.msu.edu (K. Promislow), jsp7@hawaii.edu (J. St-Pierre), wetton@math.ubc.ca (B. Wetton).

0378-7753/$ – see front matter © 2011 Elsevier B.V. All rights reserved.
doi:10.1016/j.jpowsour.2011.08.070

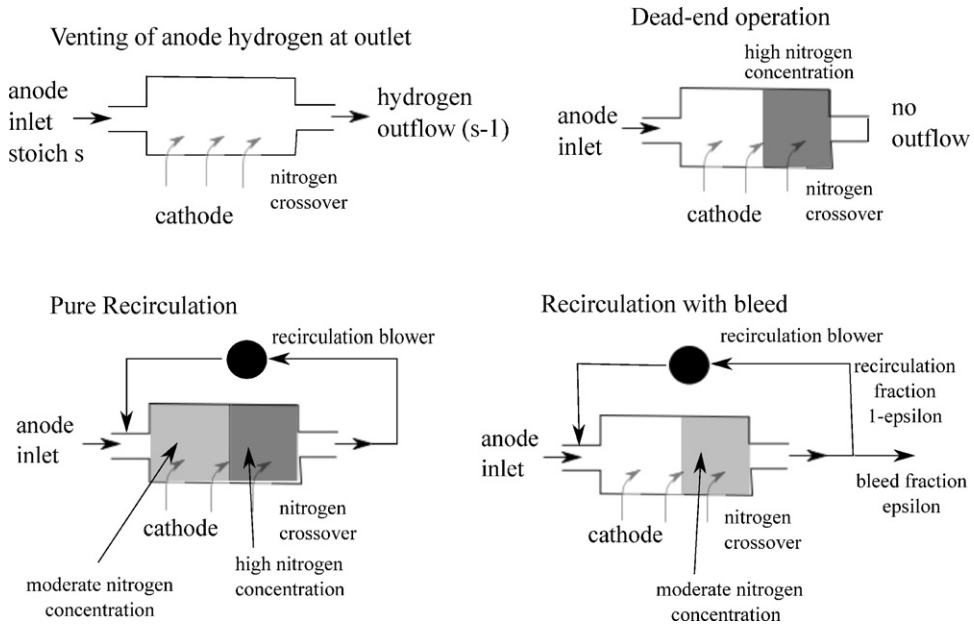

Fig. 1. Schematic comparison of anode outlet strategies.

is similar in spirit to that developed in [15]. We focus on operating current densities and exploit the scaling in this case to get approximate analytic results that we use to optimize the performance of systems using anode recirculation.

In Section 2 we present empirical models of crossover rates. The characteristic relaxation time of anode nitrogen concentrations to steady state is identified. In Section 3 we present the simplified, analytic model based on slow crossover asymptotics. The model is appropriate for straight gas channel design such as Ballard Mk 9 hardware. Variations along the channel length are considered but performance is averaged over cross-plane geometry. The model shows large anode nitrogen concentration at steady state at anode outlet. In Section 4 a strategy to reduce anode nitrogen concentrations with an anode outlet flow bleed is examined with the model. It is shown that even small bleed rates (a few per cent) can considerably reduce nitrogen levels. In the framework of the model, the relative efficiency of strategies (venting, pure recirculation and recirculation with bleed) can be investigated. Optimal bleed rates are determined in Section 5. We end with a short summary.

2. Nitrogen crossover

Experimental measurements of gas transport through Nafion show that the gas flux rate is proportional to gas concentration difference across the membrane as well as several other factors. A fit of the experimental measurements provided to us by Ballard Power Systems gives the following empirical formula for nitrogen crossover:

$$M = AK_N \frac{\Delta C}{L_m} \tag{1}$$

where M is the flow of nitrogen from cathode to anode per unit cell in mol s^{-1}, A is the unit cell active area in m^2, K_N is a fitted parameter in $m^2\ s^{-1}$ with dependence on temperature and relative humidity, ΔC is the difference in cathode to anode molar nitrogen concentration (mol m^{-3}) and L_m is the membrane thickness. In the analytical model below, we take a representative constant value of K_N from the fit to be

$$K_N = 8 \times 10^{-11}\ m^2\ s^{-1}. \tag{2}$$

Taking K_N constant is appropriate for well humidified cells where the temperature does not vary significantly. This is within a factor of two of the value estimated in [15], where a similar form to (1) for crossover is used, determined using different experimental techniques.

2.1. Recirculation-crossover time scale

In later sections, we consider the behaviour at steady state of fuel cells operated with anode recirculation, including the significant variation of anode nitrogen concentration along the channel. However, we give here a rough time scale of the transients to reach this steady state, using Ballard Mk 9 hardware as an example. We take the unit cell area to be 300 cm^2 or $3 \times 10^{-2}\ m^2$, the membrane to be Nafion 112 so thickness 50 μm. We consider the active recirculation volume to be that of the anode GDL, channels, and gas manifold and estimate

$$V \approx 32\ cm^3 = 32 \times 10^{-6}\ m^3. \tag{3}$$

Here, the manifold volume is divided by the number of cells in the stack. If the recirculation system had a significant gas volume, it should also be added to V above, also divided by the number of cells in the stack. We let $C(t)$ be the average molar concentration of nitrogen in the anode compartment assuming pure recirculation operation. Neglecting the spatial variations in this concentration from inlet to outlet that are considered below and also neglecting channel level boundary layer and mixing effects, we can derive the simple mass balance:

$$\frac{dC}{dt} = \frac{1}{V}\frac{AK_N}{L_m}(C_o - C) \tag{4}$$

where C_o is the average cathode compartment concentration of nitrogen. This gives a recirculation time scale of

$$\frac{VL_m}{AK_N} \approx 670\ s. \tag{5}$$

This time scale is sufficiently small in comparison to many car trip durations that the steady state discussion below is relevant to automotive applications. The time scale is long enough that when anode exit hydrogen is vented at operating power, nitrogen crossover

can be neglected. However at very low current densities (not considered in this work but see [15]) and in recirculation it can be significant.

3. Steady state analytic model

We consider nitrogen crossover to anode with anode recirculation under some simplifying assumptions:

1. The cathode nitrogen partial pressure is constant P_N [28].
2. The anode is isothermal and saturated and at constant pressure P_a. The partial pressure of non-vapour gases is $P_r = P_a - P_{sat}(T)$ [28].
3. The current density i is uniform. For example, at operating power for Ballard Mk 9 hardware, less than 10% deviation was observed [23].
4. The nitrogen crossover factor K_N is constant given by (2).
5. Recirculation and crossover are at steady state.

We consider a unit cell of length L_c and width W, with down-channel length parametrized by y and anode inlet at $y = 0$. We consider quantities:

$N(y)$: anode nitrogen flow (mol s^{-1}).
$P(y)$: anode nitrogen partial pressure (Pa).
$H(y)$: anode hydrogen flow (mol s^{-1}) given explicitly by

$$(sL_c - y)\frac{iW}{2\mathcal{F}} \tag{6}$$

where s is the anode stoichiometric flow rate. It is here that the assumption of uniform current density is used.

A standard flow fraction argument assuming ideal gas behaviour [6] and well-mixed gases in the channels gives:

$$P(y) = P_r \frac{N}{N+H} \tag{7}$$

and the crossover model gives

$$\frac{dN}{dy} = \alpha W(P_N - P) \tag{8}$$

where

$$\alpha = \frac{K_N}{L_m RT}. \tag{9}$$

Combining (7) and (8) we obtain

$$\frac{dN}{dy} = \alpha W P_N \left(1 - \frac{P_r}{P_N}\frac{N}{N + (sL_c - y)(iW/2\mathcal{F})}\right). \tag{10}$$

We scale $\hat{y} = y/L_c$ and

$$\hat{N} = \frac{N 2\mathcal{F}}{iWL_c} \tag{11}$$

and to obtain the scaled equation

$$\frac{d\hat{N}}{d\hat{y}} = c\left(1 - \frac{r\hat{N}}{\hat{N} + s - \hat{y}}\right). \tag{12}$$

Here $r = P_r/P_N$. We use $r \approx 4/3$ obtained from a saturated anode at 2.2 barg and a saturated cathode at 2 barg at 80% nitrogen. A higher anode pressure P_r is desirable because it minimizes the impact of nitrogen crossover as shown below. In addition, if combustion occurs it minimizes risks of propagation to the hydrogen source. The dimensionless crossover rate is

$$c = \frac{K_N}{L_m}\frac{P_N}{RT}\frac{2\mathcal{F}}{i} \approx 3 \times 10^{-3} \tag{13}$$

where we have used $i = 10,000\,\mathrm{A\,m^{-2}}$ ($1\,\mathrm{A\,cm^{-2}}$) and $P_N/R/T \approx 100\,\mathrm{mol\,m^{-3}}$. In words, c is the dimensionless number that represents the ratio of crossover to channel flows. We use the fact that c is small to simplify the model below.

Eq. (12) together with an additional boundary condition can be solved for the scaled anode nitrogen flow $\hat{N}(\hat{y})$. The boundary condition depends on the anode outlet strategy. For no recirculation (anode hydrogen is vented),

$$\hat{N}(0) = 0. \tag{14}$$

Alternatively, for pure recirculation at steady state,

$$\hat{N}(0) = \hat{N}(1). \tag{15}$$

From the solution to (12), the scaled anode nitrogen partial pressure $\hat{P}$ can be recovered:

$$\hat{P} = \frac{P}{P_r} = \frac{\hat{N}}{\hat{N} + s - \hat{y}}. \tag{16}$$

A similar model is derived in [15], in which the authors also consider hydrogen and oxygen crossover. In that work, the model is approximated numerically, and the focus is on low anode stoichiometric flow rates and low current densities. For the operating current densities considered in this paper, crossover hydrogen and oxygen (that immediately react to form water) can be neglected. It is only the unreactive nitrogen that can build to significant levels and only when it has a chance to do so in recirculation or dead end operation.

3.1. Model reduction and results

In this section we deal only with scaled quantities. We note that c (the dimensionless crossover rate) is small for operating current densities (but not necessarily at idle, see the discussion in Section 6) and expand $\hat{N}(y)$ in a regular asymptotic expansion in powers of c:

$$\hat{N}(y) = N_* + N_1(y)c + O(c^2) \tag{17}$$

where N_* is a constant (scaled) flow determined by the recirculation constraint (15). We integrate (12) from zero to one, apply the contraint keeping only $O(c)$ terms to obtain

$$\int_0^1 \left(1 - \frac{rN_*}{N_* + s - \hat{y}}\right) d\hat{y} = 0. \tag{18}$$

In physical terms this condition states that at steady state the anode nitrogen flow is approximately constant along the length of the channel and its value is such that the net crossover is zero. The integration in (18) can be done analytically leading to

$$(N_* + s - 1)e^{1/rN_*} - N_* - s = 0 \tag{19}$$

which can be solved for N_* for given operating conditions r and s. With $r = 4/3$ and $s = 1.2$ we find a root $N_* \approx 2.01$. We expect physically that there is a unique root to this equation for every $r > 1$ and $s > 1$ and observe that in our computations, but have been unable to prove this mathematically. The corresponding scaled nitrogen partial pressures from Eq. (16) are shown in Fig. 2 corresponding to the $\beta = 0$ curve. Note that the anode nitrogen partial pressures can be quite large even though the crossover rate is small (in Fig. 2 note that the scaled cathode nitrogen partial pressure is $1/r = 3/4$ and the total scaled partial pressure available to anode non-vapour gases is 1). At steady state, the net crossover rate must be zero, so the anode nitrogen partial pressure must be larger than the cathode nitrogen partial pressure in some locations. This is a significant dilution effect of anode hydrogen at outlet. Also note that the recirculation profile ($\beta = 0$) in Fig. 2 does not depend on the scaled crossover rate c as long as it is small. However, the time scale to reach steady state

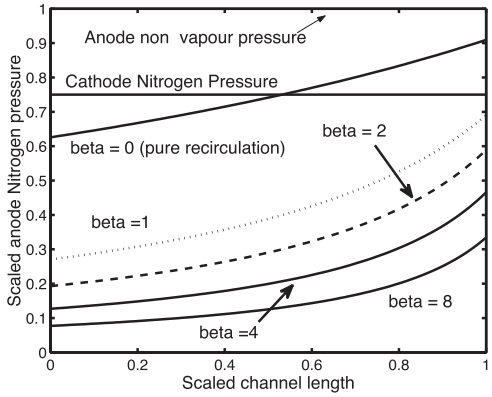

Fig. 2. Scaled anode nitrogen partial pressures for pure recirculation ($\beta = 0$) and recirculation with scaled bleed rate $\beta > 0$ at base conditions $r = 4/3$ and $s = 1.2$.

will of course depend strongly on the value of the crossover rate as discussed in Section 2.1.

This asymptotic solution structure provides clear insight into the behaviour of nitrogen concentration in recirculating cells.

4. Anode outlet bleed

The presence of crossover nitrogen in the anode can lead to a severe dilution of the hydrogen fuel concentration, as shown above. It also leads to increased demands on fuel flow pumps. Venting of exit anode gases leads to inefficiency due to fuel loss and there are safety concerns. However, since the nitrogen crossover rate was small, venting (or bleeding off) even a small fraction of the anode outlet flow would lead to a much smaller nitrogen build-up in anode recirculation [15,19,21]. This approach can be analyzed in the same approximate, analytic framework as above. If a small fraction ϵ of the outlet flow was vented then the recirculation condition (15) would become

$$\hat{N}(0) = (1 - \epsilon)\hat{N}(1). \tag{20}$$

The same fraction of hydrogen and water vapour are also vented. The losses due to the vented hydrogen are considered in the optimization study in Section 5. This condition fits into our asymptotic framework above if we take $\beta = \epsilon/c$. We find the nitrogen flow N_* to satisfy a modified version of (19):

$$N_* + s - 1 - (N_* + s)e^{(\beta/r)-(1/rN_*)} = 0. \tag{21}$$

The corresponding scaled anode nitrogen partial pressures for several values of β are shown in Fig. 2. Notice that the $\beta = 1$ curve leads to a dramatic improvement in anode nitrogen levels and corresponds to an anode outlet bleed of less than 1% by volume flow with the typical conditions considered above.

The dependence of anode nitrogen flow N_* and the scaled anode nitrogen partial pressure at anode outlet $\hat{P}(1)$ on r and s are shown in Tables 1 and 2, respectively. Note that r is restricted below by

Table 1
Scaled nitrogen flow N^* (top) and outlet scaled nitrogen partial pressure $\hat{P}(1)$ (bottom) dependence on scaled bleed rate β and ratio r of anode non-vapour partial pressure to cathode nitrogen partial pressure. Anode stoichiometric flow rate $s = 1.2$.

r	$\beta = 0$	$\beta = 1$	$\beta = 2$	$\beta = 4$
1.25	2.70	0.466	0.296	0.178
4/3	2.01	0.445	0.287	0.174
1.5	1.32	0.406	0.269	0.168
1.25	0.931	0.700	0.597	0.471
4/3	0.909	0.690	0.589	0.466
1.5	0.868	0.670	0.574	0.456

Table 2
Scaled nitrogen flow N^* (top) and outlet scaled nitrogen partial pressure $\hat{P}(1)$ (bottom) dependence on scaled bleed rate β and anode stoichiometric flow rate s. The ratio r of anode non-vapour partial pressure to cathode nitrogen partial pressure is held fixed at $r = 4/3$.

s	$\beta = 0$	$\beta = 1$	$\beta = 2$	$\beta = 4$
1.1	1.69	0.408	0.266	0.164
1.2	2.01	0.445	0.287	0.174
1.5	2.94	0.524	0.3271	0.193
1.1	0.944	0.803	0.727	0.621
1.2	0.909	0.690	0.589	0.466
1.5	0.855	0.512	0.396	0.278

$1/0.79 \approx 1.25$ in the case when both anode and cathode are saturated and at the same pressure. It is restricted above since the membrane cannot support too large a pressure difference between anode and cathode. Larger values of r could be attained if the cathode gases were oxygen enriched (nitrogen reduced) [25]. As expected, as r or s increases, the dilution effect of anode hydrogen at outlet by nitrogen becomes less severe ($\hat{P}(1)$ goes down). The anode nitrogen flow decreases as r increases and increases as s increases, also as expected. However, even moderate scaled bleed rates β make both these effects much less significant. Note that the middle lines on the bottom on both tables correspond to the values at the right of the graph in Fig. 2.

5. Optimizing efficiency with anode outlet bleed

The results in Section 4 from the asymptotic (small c) approximation agree with numerical results from the full model (12) to within 5% for the r and s values considered above and for $c = 3 \times 10^{-3}$ ($1\,\mathrm{A\,cm^{-2}}$) to $c = 3 \times 10^{-2}$ ($100\,\mathrm{mA\,cm^{-2}}$). This gives us confidence in using the reduced, analytic model to perform the following energetic optimization of anode outlet bleed rate. We assume that the overall efficiency of the cell is roughly constant over a range of operating current densities and estimate the *additional* fractional efficiency losses due to anode hydrogen recirculation with bleed strategy by the following quantity

$$\mathcal{E} = (s - 1)\beta c + \gamma N_*(\beta). \tag{22}$$

Recall that $\epsilon = \beta c$ is the actual bleed rate, so the first term above is the efficiency losses due to lost hydrogen. Here c appears in the expression above and so the results in this section will depend on its value. In the study below, we take two representative values, corresponding to $1\,\mathrm{A\,cm^{-2}}$ and $100\,\mathrm{mA\,cm^{-2}}$. If the cell were operated with no recirculation, the fractional efficiency loss would simply be approximated by $(s - 1)$. The second term above represents the efficiency losses to the compressors and pumps to recirculate the constant anode nitrogen flow. Note that the scaling is correct since N_* is an anode stoichiometric flow ratio (11). The term γ is the marginal efficiency loss to compressors and pumps for additional anode nitrogen flow measured as a stoichiometric flow rate. Following our assumption above that the efficiency of the cell is roughly constant over a range of operating current densities, it is reasonable to consider γ also constant over this range. Below, further discussion and estimates of γ are given. We demonstrate that the losses (22) can be minimized by choosing an optimal bleed rate parameter $\beta > 0$ and that the fuel cell efficiency at this optimal bleed rate is always higher than in pure recirculation ($\beta = 0$) or pure venting ($\beta c = 1$, $N_* = 0$) operation.

Our expression (22) is idealized to consider only losses to vented hydrogen and parasitic power of the additional anode nitrogen flow. Additional losses are present which are not accounted for: the lowered hydrogen concentrations due to nitrogen dilution will lead to Nernst and kinetic losses [10]. These would be enhanced by mass transport losses from channel to catalyst sites [24] and in extreme

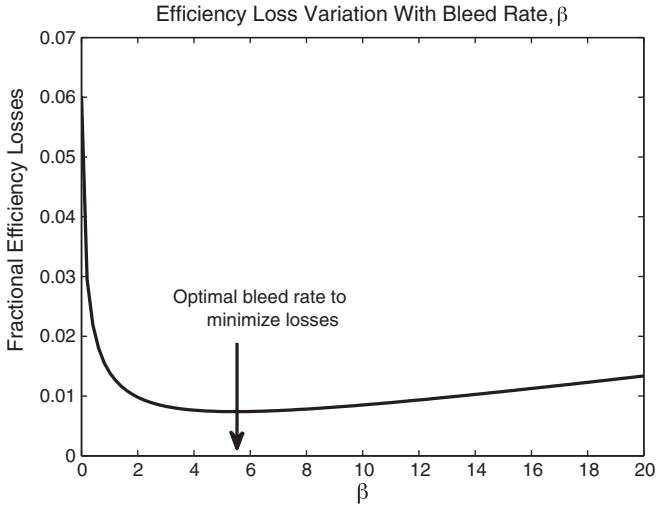

Fig. 3. Fractional efficiency losses for varied scaled bleed rates β at base conditions $r = 4/3$, $s = 1.2$, $\gamma = 0.03$, and $c = 3 \times 10^{-3}$ ($1\,A\,cm^{-2}$).

cases would lead to significant redistribution of current within the cell. These effects are outside the analytic framework of our model, and we leave them to simulation tools with more detailed physics. As a rule of thumb, our results will be approximately valid as long as

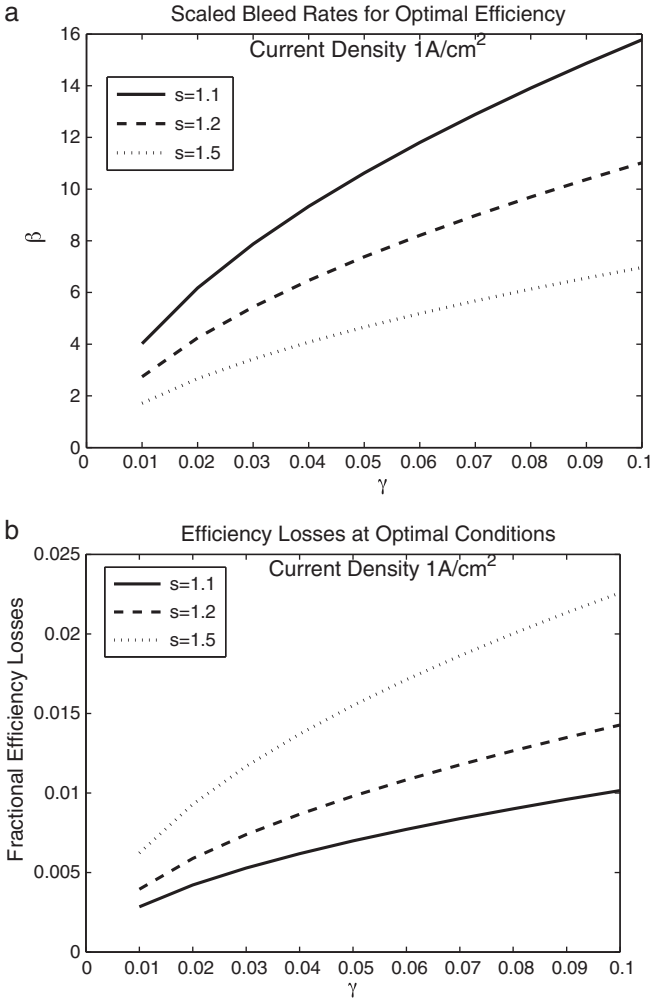

Fig. 4. Optimal bleed rates and efficiencies for $r = 4/3$ and $c = 3 \times 10^{-3}$ ($1\,A\,cm^{-2}$).

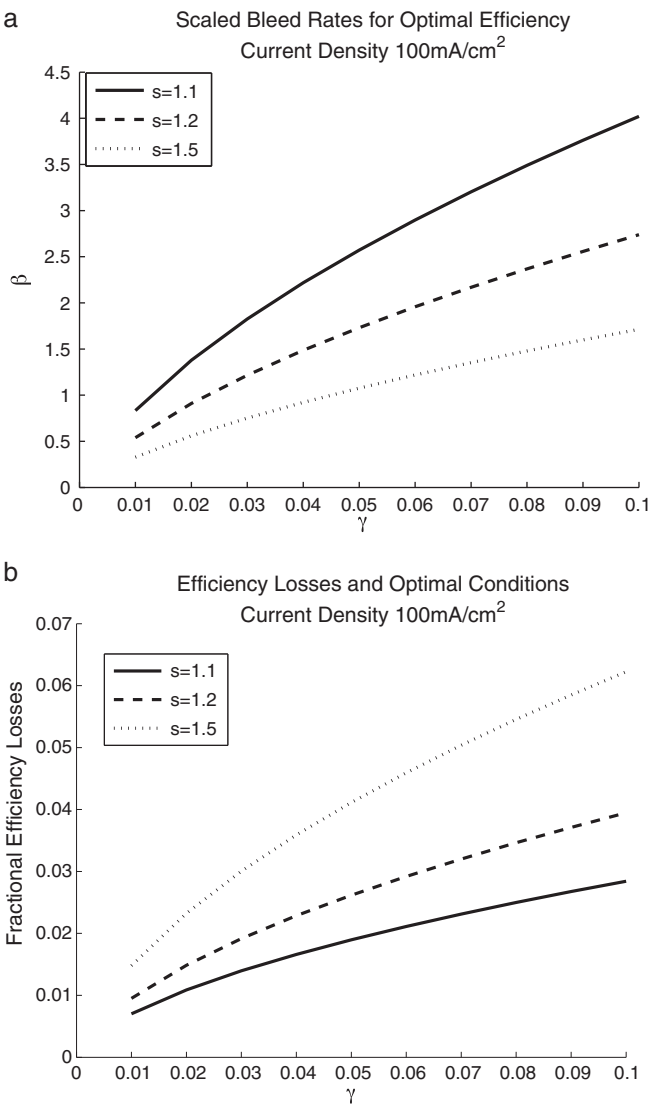

Fig. 5. Optimal bleed rates and efficiencies for $r = 4/3$ and $c = 3 \times 10^{-2}$ ($100\,mA\,cm^{-2}$).

the anode outlet scaled nitrogen concentration does not approach 1. This is true in the results shown below.

Returning to (22), we estimate the marginal compressor efficiency loss parameter γ below, beginning with an estimate of the fraction η of power generated by the cell that is lost to parasitic power for compressors and pumps without recirculation. We take $\eta = 0.15$ [11] as a base case, although a range of larger values has been reported in the literature ($\eta = 0.2$ [13] and even $\eta = 0.5$ [27] for an older, experimental stack). We note that η is not the energy *efficiency* of the pumps and compressors [7] but rather the fraction of stack output power used by these external devices. In operation without recirculation, the anode flow volume is small compared to the cathode and we neglect it in the rough estimate below. Assuming an cathode stoichiometric flow rate of s_c of air at approximately 20% oxygen, the cathode flow rate is $5s_c/2$, where the factor of 2 converts from cathode to anode stoichiometry. This leads to an estimate of

$$\gamma \approx \frac{2\eta}{5s_c} = 0.03 \tag{23}$$

using $s_c = 2$ and the base value of $\eta = 0.15$ taken above. This calculation assumes that the characteristics of the anode and cathode compressors and flow channels are similar and that the efficiency losses in these devices are linear with flow rate. There is some

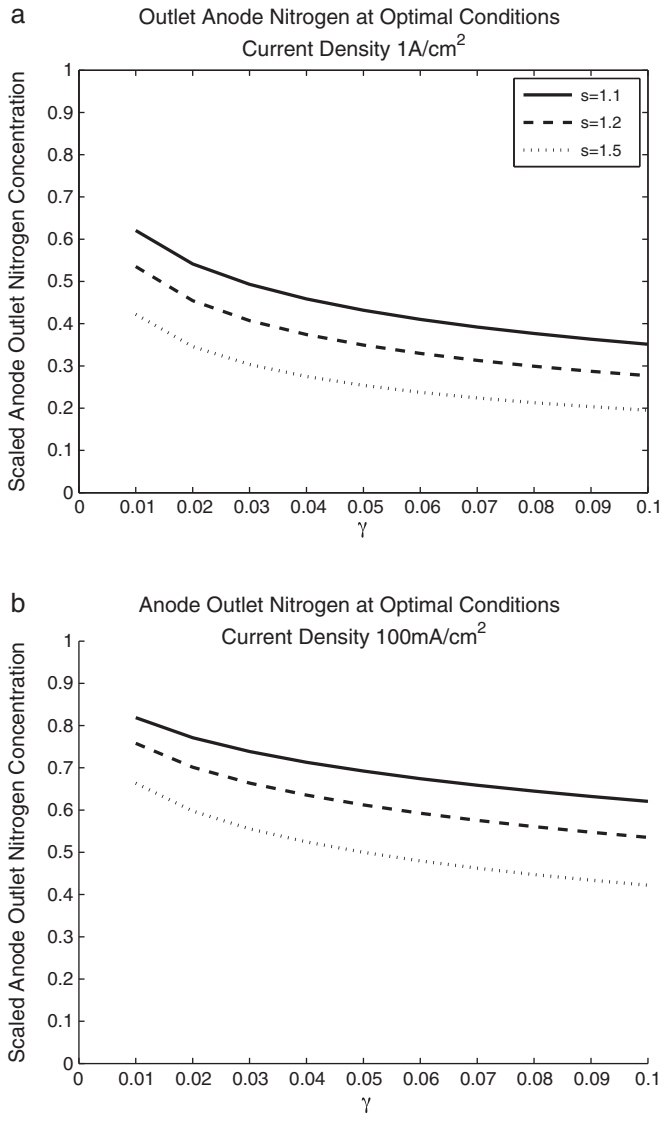

Fig. 6. Anode outlet scaled nitrogen partial pressures $\hat{P}(1)$ at optimal bleed rates for $r = 4/3$ with $c = 3 \times 10^{-3}$ ($1\,A\,cm^{-2}$) on the left and $c = 3 \times 10^{-2}$ ($100\,mA\,cm^{-2}$) on the right.

variability in the value of η between systems in the literature and some uncertainty in the assumptions made above, so we take the base value of $\gamma = 0.03$ but it also varies it in the range 0.01–0.1 in what follows. The definition of γ in this way as the marginal parasitic efficiency loss fraction allows the two terms in (22) to be considered in this simple, additive way.

In Fig. 3 we plot the fractional loss estimates (22) as a function of bleed rate β. There is a clear optimal bleed rate to minimize efficiency losses, balancing the losses due to vented hydrogen (increasing β) and parasitic losses due to increased anode nitrogen flow (decreasing β). The behaviour after the minimum loss has a small gradient, so overestimating the optimal bleed rate would still give relatively good performance. This feature also gives some room to maintain good performance when other loss mechanisms are taken into account.

Note that at this optimal bleed rate the efficiency loss of the strategy is just over 1%, while the losses to pure recirculation $\beta = 0$ are about 6% (as can be seen at the left side of Fig. 3) and for pure venting (at $s = 1.2$) are 20%. Optimizing losses (22) with respect to β requires derivatives and second derivatives of N_* with respect to β that can be found by implicit differentiation of (21). Using Newton's method, optimal bleed rates can be found for given parameters r, s, c and γ accurately and efficiently.

The optimal β values with the corresponding efficiency losses (22) are shown in Figs. 4 ($c = 3 \times 10^{-3}$ corresponding to $1\,A\,cm^{-2}$) and 5 ($c = 3 \times 10^{-2}$ corresponding to $100\,mA\,cm^{-2}$). In Fig. 6 the volume fraction of anode nitrogen at outlet $\hat{P}(1)$ is shown at these optimal conditions. As shown in Section 4, there is little variation with r when there is any significant bleed rate β so we kept $r = 4/3$ fixed for this study.

As expected, losses increase with γ, the anode compressor parasitic loss coefficient. However, this increase is sublinear because the optimal solution can trade off with hydrogen losses to bleed. The efficiency losses decrease with anode stoichiometry s as expected. Anode stoichiometry should be reduced as far as tolerances to starvation will allow. At operating power and at optimal bleed rates, efficiency losses due to recirculation with bleed are only a few percent. When comparing Figs. 4 and 5 recall that the actual bleed rate is $\epsilon = \beta c$ so at the lower current density, the optimal bleed rate is larger even though the β values are smaller. This accounts for the larger efficiency loss at the lower current density.

6. Summary and discussion

We have developed an analytic model of nitrogen crossover and build-up in a fuel cell anode in recirculation at operating power. A simple scaling argument is used to identify the characteristic time of relaxation of anode nitrogen concentration profiles to steady state. The model shows that in pure recirculation, anode hydrogen can be severely diluted by nitrogen. The model is then used to demonstrate that the technique of introducing an anode outlet flow bleed of a few percent can significantly reduce anode nitrogen concentrations.

An asymptotic version of the crossover/recirculation model is used in most of this work. This is appropriate for small scaled crossover rates c from (13). For modern membranes and operating regimes, this assumption is valid, but at low current densities (*i.e.* idling) it may not be. In low current operation, qualitative information on nitrogen concentrations can be found by solving the full equation (12) and recirculation condition (15) rather than the asymptotic version. This was the approach taken in [15] where numerical computation of a similar model including the effects of hydrogen and oxygen crossover were considered.

The crossover, recirculation and bleed effects were incorporated into a more complete unit cell computational model described in [6] that has been extensively fitted and validated to experimental data for Ballard Mk 9 hardware. These computational results are very similar to the ones from the simple, analytic model described here for operating power conditions. This gave us confidence to use the analytic model to compare losses (vented hydrogen and anode fuel compressors) at different bleed rates and anode stoichiometric flow rates. Optimal conditions that minimize the sum of these loses are found within the framework of the model, for parameters roughly corresponding to the Ballard Mk 9 design. The model and optimization analysis can be adapted to other fuel cell designs and operating conditions. Only two key parameters are needed: a nitrogen crossover coefficient and the marginal efficiency loss to compressors for increased anode gas flow.

Several simplifying assumptions have been made in the model. Most notable are the assumptions of uniform current density (anode kinetics were neglected) and the effects of water management in recirculating systems. However, the simplicity of the model allows clear insight into some of the basic elements of these systems. Other factors can be assessed in the context of these results, which can also be used to identify appropriate parameter regimes for experimental studies.

References

[1] M. Badami, M. Mura, Energy Convers. Manage. 51 (2010) 553–560.
[2] K.D. Baik, M.S. Kim, Int. J. Hydrogen Energy 36 (2011) 732–739.
[3] C. Bao, M. Ouyang, B. Yi, Int. J. Hydrogen Energy 31 (2006) 1879–1896.
[4] C. Bao, M. Ouyang, B. Yi, Int. J. Hydrogen Energy 31 (2006) 1897–1913.
[5] C. Bao, K. Zhang, M. Ouyang, B. Yi, P. Ming, J. Fuel Cell Sci. Technol. 3 (2006) 333–345.
[6] P. Berg, K. Promislow, J. St-Pierre, J. Stumper, B. Wetton, J. Electrochem. Soc. 151 (2004) A341–A353.
[7] B. Blunier, A. Miraoui, J. Fuel Cell Sci. Technol. 7 (2010) 041007 (11 pp.).
[8] R. Borup, J. Meyers, B. Pivovar, Y.S. Kim, R. Mukundan, N. Garland, D. Myers, M. Wilson, F. Garzon, D. Wood, P. Zelenay, K. More, K. Stroh, T. Zawodzinski, J. Boncella, J.E. McGrath, M. Inaba, K. Miyatake, M. Hori, K. Ota, Z. Ogumi, S. Miyata, A. Nishikata, Z. Siroma, Y. Uchimoto, K. Yasuda, K.-i. Kimijima, N. Iwashita, Chem. Rev. 107 (2007) 3904–3951.
[9] N. Bussayajarn, H. Ming, K.K. Hoong, W.Y.M. Stephen, C.S. Hwa, Int. J. Hydrogen Energy 34 (2009) 7761–7767.
[10] R. Halseid, R. Tunold, J. Electrochem. Soc. 153 (2006) A2319–A2325.
[11] K. Haraldsson, Ph.D. Thesis, KTH Chemical Engineering and Technology, 2005.
[12] S. Hikita, F. Nakatani, K. Yamane, Y. Takagi, JSAE Rev 23 (2002) 177–182.
[13] M.A. Howe, D.N. Rocheleau, J. Fuel Cell Sci. Technol. 6 (2009) 031006 (5 pp.).
[14] H. Karimaki, L.C. Perez, K. Nikiforow, T.M. Keranen, J. Viitakangas, J. Ihonen, Int. J. Hydrogen Energy 36 (2011) 10179–10187.
[15] S.S. Kocha, J.D. Yang, J.S. Yi, AIChE J. 52 (2006) 1916–1925.
[16] J. Larminie, A. Dicks, in: Fuel Cell Systems Explained, John Wiley and Sons, Ltd., 2003.
[17] G. Li, P. Pickup, Electrochim. Acta 49 (2004) 4119–4126.
[18] S. Litster, N. Djilali, Electrochim. Acta 52 (2007) 3849–3862.
[19] R.W. Lyczkowski, D. Gidaspow, AIChE J. 17 (1971) 1208–1214.
[20] E.A. Muller, F. Kolb, L. Guzzella, A.G. Stefanopoulou, D.A. McKay, J. Fuel Cell Sci. Technol. 7 (2010) 021013.
[21] J. Scholta, B. Rohland, H. Wendt, J. Appl. Electrochem. (2000) 3–331.
[22] Y. Sone, M. Ueno, H. Naito, S. Kuwajima, Electrochemistry 74 (2006) 768–773.
[23] J. St-Pierre, N. Jia, R. Rahmani, J. Electrochem. Soc. 155 (2008) B315–B320.
[24] J. St-Pierre, Fuel Cells 11 (2011) 263–273.
[25] J. St-Pierre, D.P. Wilkinson, AIChE J. 47 (2001) 1482–1486.
[26] R.C. Urian, A.F. Gulla, S. Mukerjee, J. Electroanal. Chem. 554-555 (2003) 307–324.
[27] D.P. Wilkinson, H.H. Voss, K. Prater, J. Power Sources 49 (1994) 117–127.
[28] D.P. Wilkinson, J. St-Pierre, J. Power Sources 113 (2003) 101–108.
[29] W.H. Zhu, R.U. Payne, B.J. Tatarchuk, J. Power Sources 156 (2006) 512–519.

Glossary

β: Scaled anode outlet bleed fraction. The actual bleed fraction ϵ corresponding to Fig. 1 is given by $\epsilon = \beta c$.

c: Dimensionless nitrogen crossover rate, the ratio of crossover to channel flow. Varies inversely with the current density of the cell due to the normalization, since the channel flow increases linearly with current density, see Eq. (13). The base value $c = 3 \times 10^{-3}$ corresponds to 1 A cm^{-2}.

$\mathcal{E}$: Dimensionless, fractional efficiency loss for recirculation strategies. Optimal strategies to minimize these losses are investigated in Section 5.

γ: Dimensionless parameter that represents the marginal efficiency loss of the cell operating with increased nitrogen anode flow, measured in terms of an anode stoichiometric flow. Base value $\gamma = 0.03$.

r: Dimensionless ratio of the partial pressure available to non-vapour gases in the anode to the partial pressure of nitrogen in the cathode. Base value $r = 4/3$.

s: Anode inlet stoichiometric flow rate. Base value $s = 1.2$.

$\hat{y}$: Scaled length down the cell from anode inlet $\hat{y} = 0$ to outlet $\hat{y} = 1$.

$\hat{N}(\hat{y})$: Dimensionless anode nitrogen flow, scaled as an anode stoichiometric flow.

N_*: For small values of c in recirculation, the value of $\hat{N}$ is approximately constant in $\hat{y}$. N_* denotes this constant value.

$\hat{P}(\hat{y})$: Dimensionless anode nitrogen partial pressure, scaled to the anode partial pressure available to non-vapour gases. $\hat{P} = 1$ corresponds to an anode location completely filled with saturated nitrogen.